WILEY-BLACKWELL

Full-length article

Discovery and characterization of a novel inhibitor of CDC25B, LGH00045[1]

Xu FENG[2,4], Li-na WANG[3,4], Yue-yang ZHOU[3], Hai-ping YU[3], Qiang SHEN[3], Yi ZANG[3], Yu-bo ZHOU[3], Jing-ya LI[3], Hai-xia ZHANG[2,5], Jia LI[3,5]

[2]*College of Chemistry and Chemical Engineering, Lanzhou University, Lanzhou 730000;* [3]*National Center for Drug Screening, Shanghai Institute of Materia Medica, Shanghai Institutes for Biological Sciences, Chinese Academy of Sciences, Shanghai 201203, China*

Key words

Abstract

Aim: Cell division cycle 25 (CDC25) phosphatases have recently been considered as potential targets for the development of new cancer therapeutic agents. We aimed to discover novel CDC25B inhibitors in the present study. **Methods**: A molecular level high-throughput screening (HTS) assay was set up to screen a set of 48000 pure compounds. **Results:** HTS, whose average Z´ factor is 0.55, was finished and LGH00045, a mixed-type CDC25B inhibitor with a novel structure and relative selectivity for protein tyrosine phosphatases, was identified. Furthermore, LGH00045 impaired the proliferation of tumor cells and increased cyclin-dependent kinase 1 inhibitory tyrosine phosphorylation. In synchronized HeLa cells, LGH00045 delayed cell cycle progression at the G_2–M transition. **Conclusion:** LGH00045, a novel CDC25B inhibitor identified through HTS, showed good inhibition on the proliferation of tumor cells and affected the cell cycle progression, which makes it a good hit for further structure modification.

Introduction

Cell division cycle 25 (CDC25), a subfamily of dual specificity protein-tyrosine phosphatase (DUSP), plays a pivotal role in the regulation of the cell cycle. There are 3 CDC25 homologues encoded by the human genome: CDC25A, CDC25B, and CDC25C[1]. CDC25A is involved in G_1/S phase transition through dephosphorylating the cyclin-dependent kinase 2 (CDK2)/cyclin A complex[2]. CDC25B functions as a mitotic starter by dephosphorylating and activating CDK2/cyclin A and CDK1/cyclin B[3], and CDC25C was thought to be involved in permitting cell entry into mitosis and controlling the initiation of the S-phase[4]. In addition, CDC25 phosphatases are involved in mitogenic and steroid receptor signal transduction pathways and apoptotic responses to stress[5].

CDC25 phosphatases, particularly the CDC25A and CDC25B isoforms, have been reported to be overexpressed in primary tissue samples from various human cancers[6–11]. Several lines of evidence indicate that the overexpression of CDC25 contributes to cancer. The co-expression of CDC25A or CDC25B cooperated with either oncogenic v-Ha-ras Harvey rat sarcoma viral oncogene homolog (HRAS) or the loss of retinoblastoma (RB1) gene to transform mouse embryonic fibroblasts, which resulted in the capability of forming high-grade tumors *in vivo*[12]. Furthermore, the targeting of CDC25B overexpression to the mammary glands of mice resulted in the increased proliferation of mammary epithelial cells and hyperplasia, which induced tumor growth with additional challenge with the 9,10-dimethyl-1,2-benzanthracene carcinogen[13,14]. Conversely, downregulating the expression of CDC25B or CDC25C by microinjecting antibodies against CDC25B or CDC25C, or transfecting with inactive mutants, caused a G_2 arrest[15–17], whereas those against CDC25A caused G_1 arrest[18,19]. These results in turn make them ideal targets for a new anticancer therapy. Recent reports have shown that the most numerous and active inhibitors were paraquinonoid compounds derived from vitamin K, such as NSC663284, JUN1111, BN82685, and adociaquinone. However, the

compounds of this family probably acted through the irreversible oxidation of the cysteine residue in the catalytic domain of CDC25 phosphatases into a sulfonic acid[20], which could cause many other off-target effects *in vivo*. Therefore, the discovery of other non-quinonoid compounds may offer new inspiration in designing CDC25B inhibitors. Some non-quinonoid CDC25 inhibitors have been published previously. For example, H32, a sulfone derivative of vitamin K3, is not capable of undergoing redox cycling and generating toxic oxygen species, compared with quinine derivatives[21]. KR61170, a 11-arylbenzo[b]naphtha[2,3-d]furan derivative, previously reported to be a potent protein tyrosine phosphatase 1B (PTP1B) inhibitor[22], was thought to interfere with the arginine residue within the catalytic domain of CDC25 proteins[23].

Due to the great potential of CDC25 as an antitumor target, a high-throughput screening (HTS) for CDC25B inhibitors based on the molecular level was developed. After the screening of our compound library, LGH00045, as a novel non-quinonoid inhibitor of CDC25B, was identified.

Materials and methods

Materials and instruments The plasmid pGEX–KG was a kind gift from Dr Kun-liang GUAN of the University of Michigan (Ann Arbor, MI, USA). The restriction enzymes and Ex *Taq* polymerase were purchased from TaKaRa (Dalian, China). *Escherichia coli* strain BL21–CodonPlus (DE3) was from Stratagene (La Jolla, CA, USA). Substrate *p*-nitrophenyl phosphate (*p*NPP) was from Calbiochem (San Diego, CA, USA), and 3-*O*-methylfluorescein phosphate (OMFP) was from Sigma (St Louis, MO, USA). High-glucose Dulbecco's modified Eagle's medium (HG-DMEM), McCoy's 5A medium, and RPMI-1640 medium were from Invitrogen (Carlsbad, CA, USA). Fetal bovine serum (FBS) was purchased from Hyclone (Logan, UT, USA). 3-(4, 5-dimethylthiazol-2-yl)-2,5-diphenyltetrazoliom bromide (MTT) and propidium iodide were also from Sigma (USA). Antibodies specific to CDK1, Y15-p CDK1 and cyclin B1, anti-β-actin, horseradish peroxidase (HRP)-linked antimouse immunoglobulin (IgG), and antirabbit IgG antibodies were purchased from Cell Signaling Technology (Danvers, MA, USA). The nitrocellulose membranes were from Amersham Biosciences (Piscataway, NJ, USA), and the enhanced chemiluminescence (ECL) reagents were from Calbiochem (USA). Other solvents and reagents used in experiments were of analytical grade.

PCR was performed using the GeneAmp PCR System2400 from Perkin–Elmer (Norwalk, CT, USA).

GSTrap FF and HiPrep 26/10 desalting columns were obtained from Amersham Pharmacia Biotech (Sweden). The continuous kinetic monitoring of enzyme activity was performed on a SPECTRAmax 340 or Flexstation2-384 microplate reader (Molecular Devices, Sunnyvale, CA, USA) and controlled by Softmax software (Sunnyvale, CA, USA). Liquid handling for random screening was carried out with a Biomek FX liquid handling workstation from Beckman Coulter (Fullerton, CA, USA) and HYTRA-96 semi-automated 96-channel pipettors from Robbins (Sunnyvale, CA, USA). A Becton Dickinson FACSCalibur CellSorting system (BD Bioscience, Franklin Lakes, NJ, USA) was also used for cell circle analysis.

Construction, expression, and purification of the CDC25B catalytic domain The cDNA of the CDC25B catalytic domain (1354–1923 nt according to gi11641416) was cloned into the pGEX–KG expression vector. The protein was expressed as a glutathione-S-transferase (GST) fusion protein in *Escherichia coli* BL21–CodonPlus (DE3) and purified with a glutathione sepharose column as previously described[24].

CDC25B enzymatic assay and HTS The enzymatic activity of the CDC25B was determined at 30 °C by monitoring the dephosphorylation of OMFP, which was detected at a 485 nm excitation wavelength and 530 nm emission wavelength in the EnVision multilabel plate reader (Perkin–Elmer Life Sciences, Boston, MA, USA). The typical inhibition assay was carried out in a 100 μL system containing 50 mmol/L Tris-HCl, pH 8.0, 50 mmol/L NaCl, pH 8.0, 10 μmol/L OMFP, 100 nmol/L recombinant CDC25B, 1 mmol/L dithiothreitol (DTT), 1 mmol/L EDTA, 1% glycerin, and 2 mg/L individual compound. The inhibition activity of the compound was continuously monitored, and the initial rate of the dephosphorylation was determined using the early linear region of the enzymatic reaction kinetic curve. The HTS finished with 48 000 pure chemicals collected from different sources with wide structural diversity according to previously described procedures[24]. Na_3VO_4 and DMSO were used as positive and negative controls, respectively, to evaluate the HTS system.

For calculating the half maximal inhibitory concentration (IC_{50}), inhibition assays were performed with 100 nmol/L recombinant enzyme in a 100 μL system containing 50 mmol/L Tris-HCl, pH 8.0, 50 mmol/L NaCl, pH 8.0, 10 μmol/L OMFP, 1 mmol/L DTT, 1 mmol/L EDTA, 1% glycerin, and the inhibitors diluted around the estimated IC_{50} values. IC_{50} was calculated from the non-linear curve fitting of the percentage of inhibition (% inhibition) versus the inhibitor concentration [I] by using the following equa-

tion % Inhibition=100/(1+[IC$_{50}$/[I]]k), where k is the Hill coefficient.

Characterization of LGH00045 To investigate the reversibility of the inhibition of LGH00045 against CDC25B, a dialysis assay was performed. Briefly, LGH00045 (9 μmol/L, approximately 10 times the IC$_{50}$) was pre-incubated at 4 °C in assay buffer containing 200 nmol/L enzyme for 30 min. The mixture (1 mL) was then dialyzed against 5000-fold of the assay buffer. CDC25B activity was determined after dialysis for 2 and 4 h. The residual activities related to the control (DMSO) were used to evaluate the reversibility of the inhibition.

To calculate the Michaelis constant K_m and the catalytic rate constant k_{cat} values of CDC25B at different concentration of LGH00045, the enzymatic assays with 2-fold diluted OMFP (from 160 μmol/L) in typical assay buffer were carried out. The Lineweaver–Burk plot was also described to evaluate the inhibition pattern.

Selectivity of LGH00045 on other PTPase family members CDC25A and some other PTPase family members, including phosphatase of regenerating liver-3 (PRL-3), Jun amino-terminal kinase stimulatory phosphatase-1 (JSP-1), leukocyte common antigen (CD45), protein tyrosine phosphatase 1B (PTP1B), and vaccinia virus H1-related dual-specific protein phosphatase (VHR) were chosen to evaluate the selectivity of LGH00045. The cDNA of CDC25A (1373–1939 nt according to gi33873622), PRL-3 (335–856 nt according to gi14589855), JSP-1 (443–991 nt according to BC022847), CD45 (1698–3791 nt according to gi115385976), PTP1B (91–1053 nt according to gi190741), and VHR (56–613 nt according to BC002682) were cloned, expressed, and purified as CDC25B The individual PTPase enzyme activity assay was performed at the optimal pH. OMFP was used as a substrate for the CDC25A, CDC25B, JSP-1, VHR, and PRL-3 assays. *p*NPP was used for PTP1B and CD45, which could generate *p*-nitrophenyl (*p*NP). The level of *p*NP was monitored at an absorbance of 405 nm by the EnVision multilabel plate reader.

Cell culture HeLa, HCT116, and MDA-MB-435S cells, purchased from American Type Culture Collection (Rockville, MD, USA), were kept at logarithmic growth in 5% CO$_2$ at 37 °C with HG-DMEM, McCoy's 5A medium, and RPMI-1640 medium, respectively, supplemented with 10% FBS and 100 units/mL each of penicillin G and streptomycin.

Cytotoxicity/proliferation assay Tumor cells were seeded onto a 96-well plate at a concentration of 2000 cells/well and incubated at 37 °C in 5% CO$_2$ for 24 h. A range of concentrations of the test compounds were added and the plate was incubated at 37 °C for 72 h before 40 μL MTT (5 mg/mL)/well was added. After 3 h incubation, the medium was removed and 100 μL DMSO was added to each well. The absorbance was measured on the Spectra-Max 340 microplate reader at a wavelength of 550 nm with a reference wavelength of 690 nm. The optical density of the result in MTT assay was directly proportional to the number of viable cells.

Flow cytometric analysis Cells were harvested by trypsin digestion, washed twice with cold phosphate-buffered saline (PBS), suspended in cold 70% ethanol, and incubated at 4 °C overnight. The cells were stained with a PBS solution containing 20 μg/mL propidium iodide and 200 μg/mL RNase A and analyzed with a Becton Dickinson FACSCalibur CellSorting system. The experiment was repeated at least 3 independent times. Cells treated with the vehicle, 1% DMSO, served as negative controls.

Western blotting Cells were rinsed twice with PBS and then lysed with 1×SDS loading buffer. The samples were electrophoresed on 10% SDS–polyacrylamide gels and transferred to nitrocellular membranes. The membranes were blocked for 1 h with 5% (*w/v*) bovine serum albumin and incubated with the primary antibodies overnight at 4 ºC and the secondary antibodies for 1 h at room temperature. Antigen–antibody complexes were detected with the ECL kit.

Statistical analysis Data are presented as mean±SEM. Statistical analysis of the data for multiple comparisons was performed by ANOVA. For single comparisons, the significance of differences between means was determined by *t*-test. A value of *P*<0.05 was considered statistically significant, and a value of *P*<0.001 was considered statistically most significant.

Results

Discovery of a novel inhibitor of CDC25B through HTS To find novel, small molecule inhibitors, a HTS with recombinant CDC25B was developed. The screening assay, consisting of 100 nmol/L GST–fusion CDC25B protein and 10 μmol/L OMFP substrate, was optimized to obtain a good signal-to-noise ratio. The intraplate and interplate coefficient of variation (CV) were both less than 10%, suggesting that the liquid handling and compound transfer procedure was precise, whereas the Z´ factor, a standard statistical measure of assay quality, was 0.55, above the routine threshold of 0.5. A total of 48 000 compounds were screened in automated format in 1 d. Fifteen

compounds with an inhibition rate higher than 50% at a final concentration of 2 µg/mL were identified.

After the hit validation and dose–response curve determination, compound LGH00045 with a novel structure (Figure 1A, chemical name: (E)3-(2-chlorophenyl)-6-(2-(furan-2-yl)vinyl)-[1,2,4]triazolo[3,4-b][1,3,4]thiadiazole) was discovered to be a potent CDC25B inhibitor with an IC_{50} of 0.82 µmol/L (Figure 1B)
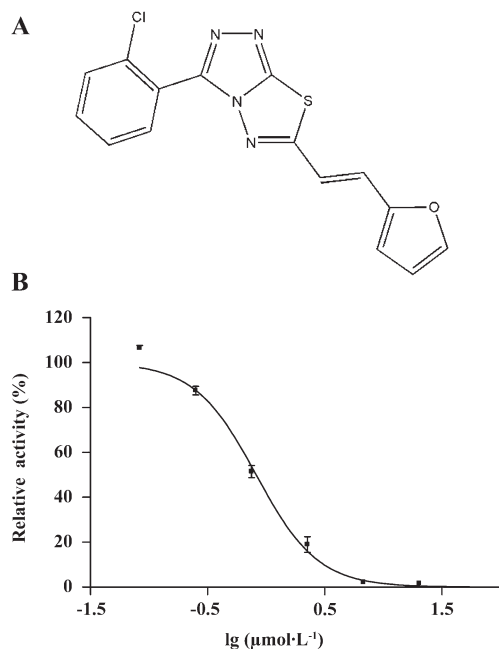

Figure 1. (A) structure of LGH00045. (B) dose-dependent inhibition of CDC25B by LGH00045.

LGH00045 inhibited CDC25B in a mixed inhibition pattern The inhibition modality of LGH00045 for CDC25B was further determined. Whether the effect of LGH00045 was reversible was first investigated. The reversibility of inhibition was determined by measuring the recovery of enzymatic activity after dialysis of the enzyme–inhibitor complex. As shown in Figure 2A, after dialysis for 4 h, the relative activity of CDC25 was approximately 4-fold that of non-dialysis, which suggested that LGH00045 was a reversible inhibitor of CDC25B.

However, when the inhibitor concentration increased, the K_m values increased, while the k_{cat} values decreased (Figure 2B), which indicated LGH00045 inhibited CDC25B in a mixed inhibition pattern. The result of the Lineweaver–Burk plot also confirmed this (Figure 2C).

Inhibitory effect of LGH00045 on other PTPase family members To test the selectivity of the compound
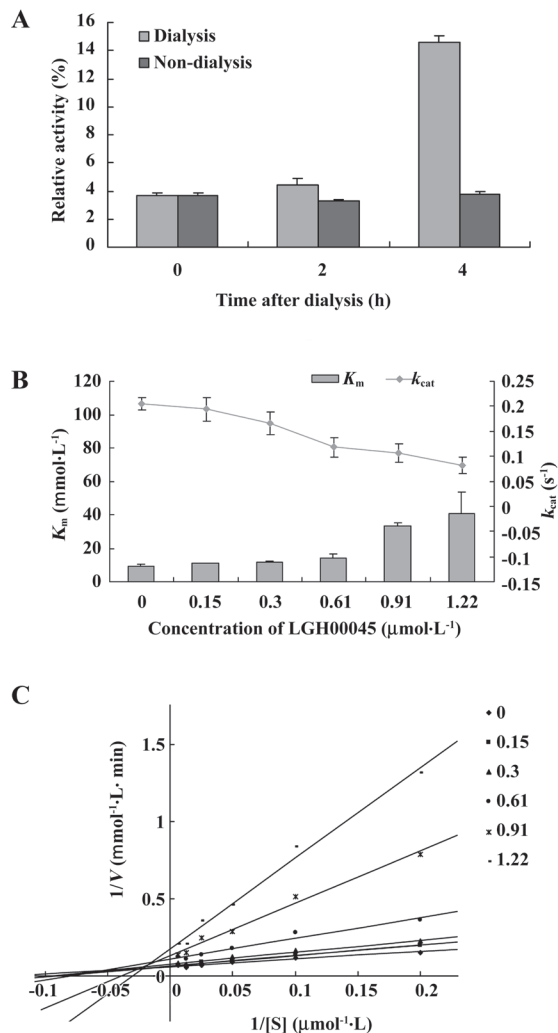

Figure 2. Characterization of LGH00045 to CDC25B. (A) reversibility of compound LGH00045 inhibition to CDC25B. Enzyme–inhibitor complex, including 200 nmol/L CDC25B and excessive compound LGH00045, was dialyzed against 5000-fold of the assay buffer for the indicated period of time. At the end of each dialysis, CDC25B activity was determined in a functional assay. (B) K_m and k_{cat} values at various fixed concentrations of LGH00045. K_m and k_{cat} values were obtained by non-linear curve fitting of the Michaelis–Menten equation. (C) mixed-type inhibition of LGH00045 shown by Lineweaver–Burk plot.

on other PTPase family members, we determined the IC_{50} values of LGH00045 for CDC25A, PRL-3, JSP-1, CD45, PTP1B, and VHR. The results are shown in Table 1. LGH00045 showed better inhibition on CDC25 than that on the other determined PTPase family members. The IC_{50} value of LGH00045 against CDC25A was 0.53±0.02 µmol/L, which was close to that against CDC25B (0.82±0.08 µmol/L). However, it was less than that against PRL-3 (2.49±0.30 µmol/L), VHR (5.21±0.66 µmol/L), JSP1

Table 1. IC_{50} values of LGH00045 against recombinant human CDC25B, CDC25A, PRL-3, JSP1, CD45, PTP1B and VHR. Mean±SEM. $n=3$.

PTPases	IC_{50} (µmol/L)
CDC25B	0.82±0.08
CDC25A	0.53±0.02
PRL-3	2.49±0.30
JSP1	4.66±0.53
CD45	14.90±2.04
PTP1B	5.00±0.24
VHR	5.21±0.66

(4.66±0.53 µmol/L), and PTP1B (5.00±0.24 µmol/L). It shows much more selectivity for CDC25B when compared to CD45 (14.90±2.04 µmol/L).

LGH00045 inhibited cell proliferation and induced cell cycle arrest To determine whether LGH00045 could exert the effect of CDC25B inhibitor at the cellular level, the effect of LGH00045 on tumor cell proliferation was detected. Cells were seeded at 1000 cells/well on a 96-well microplate. After 24 h, cells were treated with the indicated concentrations of LGH00045 and 1% DMSO for 72 h. Then the viability of cells was evaluated by the MTT method. As shown in Figure 3A, LGH00045 could remarkably inhibit the proliferation of MDA-MB-435S (IC_{50}: 29.24±1.28 µmol/L), HeLa (IC_{50}: 26.61±1.15 µmol/L), and HCT116 (IC_{50}: 39.81±1.85 µmol/L).

Due to the prominent role of CDC25B in controlling mitosis, the ability of LGH00045 on cell progression was examined. HeLa cells were plated on a 6-well plate at $1.5×10^4$ cells/well. After being cultured for 24 h, the cells were synchronized in the late G_1 phase by double thymidine block and released for 8 h. The synchronized cells were treated with the indicated concentration of LHG00045 and nocodazole or 1% DMSO for 10 h. After double thymidine block and release for 8 h, HeLa cells were fully synchronized with approximately 88% of the population displaying G_2/M phase DNA content. Another 10 h after release, the cells treated with increasing concentrations of LGH00045 in the G_2/M phase were blocked in the G_2/M phase in a dose-dependent manner, whereas the DMSO-treated control cells were able to complete mitosis within 10 h and undergo the following cell cycle (Figure 3B).

LGH00045 inhibited CDK1 dephosphorylation and delayed entry into mitosis CDC25B is known to play an essential role in the control of CDK activity at mitosis.
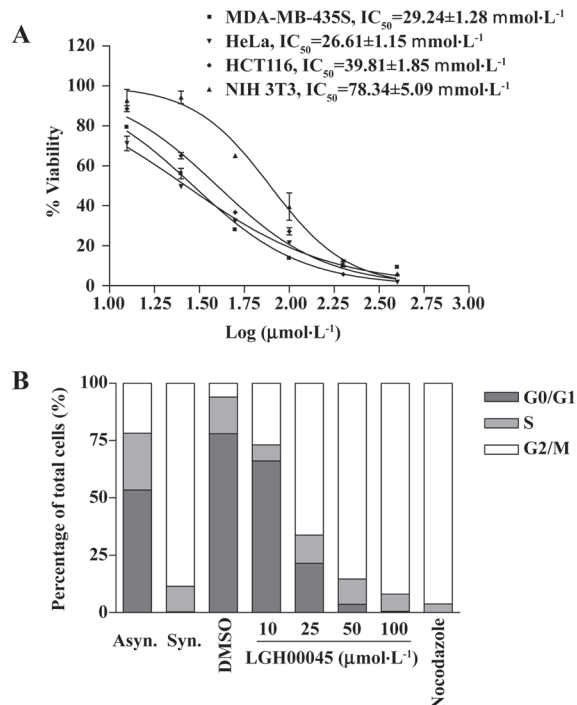

Figure 3. Proliferation arrest caused by LGH00045. (A) viability of three cancer cell lines studied by MTT after being treated with the indicated concentrations of LGH00045 for 3 d. (B) LGH00045 causes G_2/M phase arrest on HeLa cells. Asynchronous cells (Asyn) were synchronized at the G_2/M phase (Syn) and then treated LGH00045 and 0.333 µmol/L nocodazole. Cells treated with 1% DMSO were used as negative controls. Cells were then harvested and subjected to flow cytometry analysis of their DNA content after propidium iodide staining. Data were collected on a Becton Dickinson FACSCalibur and analyzed using Modfit software.

Therefore, the phosphorylation of CDK1 on tyrosine 15 was examined by Western blotting. As described earlier, HeLa cells were synchronized at the G_2/M phase and treated with LGH00045 or 1% DMSO. After 4 h, the cells were harvested for Western blotting. As shown in Figure 4, the effect of LGH00045 on the phosphorylation of CDK1 was concentration dependent. The expression level of cyclin B1 was also examined in the same experiment by Western blotting. Cyclin B1 protein accumulated with the increase of LGH00045, which indicated that cells were prevented from entering mitosis by the inhibition of CDC25B. Together, these observations suggested that CDC25B was probably the key target of the novel compound LGH00045 at the cellular level.

Discussion

CDC25 phosphatases have recently been considered as potential targets for the development of new cancer
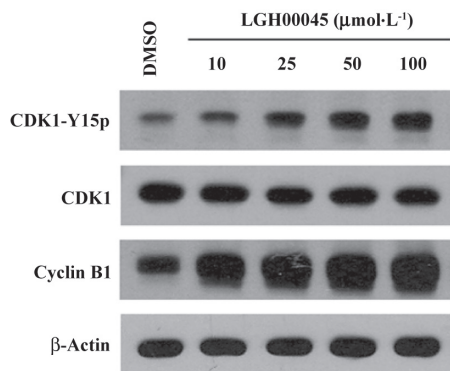
Figure 4. LHG00045 inhibited CDK1 tyrosine 15 dephosphorylation and delayed entry into mitosis. Cells in the G2/M phase were treated with the indicated concentration of LGH00045 and DMSO for 4 h and then harvested. Samples were processed for Western blot analysis.

therapeutic agents. A number of recent reports have found that the collective drug discovery effort has been directed towards the identification of novel CDC25 inhibitors that work *in vitro* and in cultured cells, and are even active against human tumors *in vivo*[1,25,26]. In this report, a credible HTS assay for CDC25B was established to discover small molecule inhibitors, whose average Z' factor is above the threshold of 0.5. This assay provided us with a powerful tool to screen a total of 48 000 pure chemicals collected from different sources with wide structural diversity.

Through large-scale screening, several hits with good activity and novel structures were discovered. Here, compound LGH00045 was reported for the first time as a novel CDC25B inhibitor. Further analysis demonstrated that it was a mixed-type, reversible inhibitor of CDC25B, which may provide us with new inspiration in further identifying its binding site and designing novel CDC25B inhibitors.

Selectivity may be the greatest problem in the development of PTPase inhibitors. Therefore, the inhibitory effect of LGH00045 on different types of PTPase was measured. The IC$_{50}$ value of LGH00045 against the other three DUSP, PRL-3, JSP-1, and VHR, and a classical non-receptor type PTPase, PTP1B, was 3-6 fold that of those against CDC25B. A classical receptor type PTPase, CD45, was approximately 17-fold. There was no evident difference between the ability of LGH00045 in inhibiting CDC25A and CDC25B. Their effects on other PTPases should be studied further to allow further modification on this scaffold to produce more potent and more selective inhibitors of individual PTPases.

It is widely known that CDC25B plays an important role in cell circle progression and cell proliferation control, and it has been regarded as a potential anticancer target.

We first investigated the antigrowth effect of LGH00045 on 3 cancer cell lines: MDA-MB-435S, HeLa, and HCT116. The results showed that LGH00045 had a similar IC$_{50}$ on the 3 cell lines, which was approximately 30 µmol/L. This proved that LHG00045 was able to inhibit cell growth as other CDC25B inhibitors did.

Whether the proliferation inhibition of LGH00045 on tumor cell lines depended on CDC25B inhibition as it did at the molecular level was further investigated. It was widely testified that CDC25B was involved in the G$_2$/M transition by dephosphorylating tyrosine 14 and 15 phosphorylation of CDK1 and activating it. Thus the inhibition of the cellular activity of CDC25B could cause G$_2$/M phase arrest[20]. Cell cycle progression after the treatment with LGH00045 was analyzed. The results showed that LGH00045 was able to arrest the cell cycle of HeLa cells in the G$_2$/M phase in a dose-dependent manner and dramatically increase tyrosine 15 phosphorylation of CDK1 in a dose-dependent manner. Simultaneously, cyclin B1 accumulated in a dose-dependent manner after LGH00045 treatment. The results suggested that LGH00045 could prevent cells from entering mitosis due to CDC25B inhibition.

In summary, a novel inhibitor of CDC25B, LGH00045, was discovered through well-controlled HTS and it could inhibit CDC25B not only *in vitro*, but also in cultured cancer cells. LGH00045 showed good inhibition to the proliferation of tumor cells and affected cell cycle progression, which makes it a good hit for further structure modification.

Author contribution

Prof Jia LI and Prof Hai-xia ZHANG designed research; Xu FENG, Li-na WANG, Yue-yang ZHOU, Haiping YU, and Qiang SHEN performed research; Yi ZANG, Yu-bo ZHOU, and Jing-ya LI analyzed data; Xu FENG and Prof Jia LI wrote the paper.

References

1 Cao S, Foster C, Brisson M, Lazo JS, Kingston DG. Halenaquinone and xestoquinone derivatives, inhibitors of CDC25B phosphatase from a *Xestospongia* sp. Bioorg Med Chem 2005; 13: 999–1003.

2 Mailand N, Falck J, Lukas C, Syljuåsen RG, Welcker M, Lukas J. Rapid destruction of human CDC25A in response to DNA damage. Science 2000; 288: 1425–9.

3 Nilsson I, Hoffmann I. Cell cycle regulation by the CDC25 phosphatase family. Prog Cell Cycle Res 2000; 4: 107–14.

4 Turowski P, Franckhauser C, Morris MC, Vaglio P, Fernandez A, Lamb NJ. Functional CDC25C dual-specificity phosphatase is required for S-phase entry in human cells. Mol Biol Cell 2003; 14:

2984–98.

5 Lyon MA, Ducret AP, Wipf P, Lazo JS. Dual-specificity phosphatases as targets for antineoplastic agents. Nat Rev Drug Discov 2002; 1: 961–76.

6 Cangi MG, Cukor B, Soung P, Signoretti S, Moreira G Jr, Ranashinge M, *et al*. Role of the CDC25A phosphatase in human breast cancer. J Clin Invest 2000; 106: 753–61.

7 Broggini M, Buraggi G, Brenna A, Riva L, Codegoni AM, Torri V, *et al*. Cell cycle-related phosphatases CDC25A and B expression correlates with survival in ovarian cancer patients. Anticancer Res 2000; 20: 4835–40.

8 Ngan ES, Hashimoto Y, Ma ZQ, Tsai MJ, Tsai SY. Overexpression of CDC25B, an androgen receptor coactivator, in prostate cancer. Oncogene 2003; 22: 734–9.

9 Sasaki H, Yukiue H, Kobayashi Y, Tanahashi M, Moriyama S, Nakashima Y, *et al*. Expression of the CDC25B gene as a prognosis marker in non-small cell lung cancer. Cancer Lett 2001; 173: 187–92.

10 Talvinen K, Tuikkala J, Grönroos J, Huhtinen H, Kronqvist P, Aittokallio T, *et al*. Biochemical and clinical approaches in evaluating the prognosis of colon cancer. Anticancer Res 2006; 26: 4745–51.

11 Sato Y, Sasaki H, Kondo S, Fukai I, Kiriyama M, Yamakawa Y, *et al*. Expression of the CDC25B mRNA correlated with that of N-myc in neuroblastoma. Jpn J Clin Oncol 2001; 31: 428–31.

12 Galaktionov K, Lee AK, Eckstein J, Draetta G, Meckler J, Loda M, *et al*. CDC25 phosphatases as potential human oncogenes. Science 1995; 269: 1575–7.

13 Ma ZQ, Chua SS, DeMayo FJ, Tsai SY. Induction of mammary gland hyperplasia in transgenic mice over-expressing human CDC25B. Oncogene 1999; 18: 4564–76.

14 Yao Y, Slosberg ED, Wang L, Hibshoosh H, Zhang YJ, Xing WQ, *et al*. Increased susceptibility to carcinogeninduced mammary tumors in MMTV- CDC25B transgenic mice. Oncogene 1999; 18: 5159–66.

15 Millar JB, Blevitt J, Gerace L, Sadhu K, Featherstone C, Russell P. p55CDC25 is a nuclear phosphoprotein required for the initiation of mitosis in human cells. Proc Natl Acad Sci USA 1991; 88: 10 500–4.

16 Lammer C, Wagerer S, Saffrich R, Mertens D, Ansorge W, Hoffmann I. The CDC25B phosphatase is essential for the G2/M phase transition in human cells. J Cell Sci 1998; 111: 2445–53.

17 Gabrielli BG, De Souza CP, Tonks ID, Clark JM, Hayward NK, Ellem KA. Cytoplasmic accumulation of CDC25B phosphatase in mitosis triggers centrosomal microtubule nucleation in HeLa cells. J Cell Sci 1996; 109: 1081–93.

18 Hoffman I, Draetta I, Karsenti G. Activation of the phosphatase activity of human CDC25A by a CDK2-cyclin E dependent phosphorylation at the G1/S transition. EMBO J 1994; 13: 4302–10.

19 Jinno S, Suto K, Nagata A, Igarashi M, Kanaoka Y, Nojima H, *et al*. CDC25A is a novel phosphatase functioning early in the cell cycle. EMBO J 1994; 13: 1549–56.

20 Boutros R, Lobjois V, Ducommun B. CDC25 phosphatases in cancer cells: key players? Good targets? Nature Reviews Cancer 2005; 7: 495–507.

21 Kar S, Wang M, Ham SW, Carr BI. H32, a nonquinone sulfone analog of vitamin K3, inhibits human hepatoma cell growth by inhibiting Cdc25 and activating ERK. Cancer Biol Ther 2006; 5: 1340–7.

22 Wrobel J, Sredy J, Moxham C, Dietrich A, Li Z, Sawicki DR, *et al*. PTP1B inhibition and antihyperglycemic activity in the ob/ob mouse model of novel 11-arylbenzo[b]naphtho[2, 3-d]furans and 11-arylbenzo[b]naphtho[2, 3-d]thiophenes. J Med Chem 1999; 42: 3199–202.

23 Cheon HG, Kim SM, Yang SD, Ha JD, Choi JK. Discovery of a novel protein tyrosine phosphatase-1B inhibitor, KR61639: potential development as an antihyperglycemic agent. Eur J Pharmacol 2004; 485: 333–9.

24 Shi L, Yu HP, Zhou YY, Du JQ, Shen Q, Li JY, *et al*. Discovery of a novel competitive inhibitor of PTP1B by high-throughput screening. Acta Pharmacol Sin 2008; 29: 278–84.

25 Brezak MC, Quaranta M, Contour-Galcera MO, Lavergne O, Mondesert O, Auvray P, *et al*. Inhibition of human tumor cell growth *in vivo* by an orally bioavailable inhibitor of CDC25 phosphatases. Mol Cancer Ther 2005; 4: 1378–87.

26 Brisson M, Nguyen T, Vogt A, Yalowich J, Giorgianni A, Tobi D, *et al*. Discovery and characterization of novel small molecule inhibitors of human CDC25B dual specificity phosphatase. Mol Pharmacol 2004; 66: 824–33.